MICRO-JET NOZZLE ARRAY FOR PRECISE DROPLET METERING AND STEERING HAVING INCREASED DROPLET DEFLECTION

Constantine N. Anagnostopoulos, James M. Chwalek, Christopher N. Delametter, Gilbert A. Hawkins, David L. Jeanmaire, John A. Lebens, Ali Lopez, and David P. Trauernicht
Research & Development Laboratories, Eastman Kodak Company
Rochester, NY 14650-2121 USA

ABSTRACT

We present the architecture and fabrication method of a fluidic device with increased droplet deflection. The device is capable of producing picoliter size droplets precisely and steering them. The precision is a consequence of the reproducibility of the nozzles that are made using VLSI technology and tools. In addition, the droplet size is determined by the precise timing of applied heat pulses. We present both experimental and modeling results.

INTRODUCTION

We recently reported the design of a novel CMOS/MEMS, high-speed, micro-jet, nozzle array device capable of precise metering and steering of fluids [1,2]. The device can be used for high-speed inkjet printing as well as other applications. It consists of an array of nozzles, each surrounded by a heater. The heater is split into two semicircular portions, as shown in Fig. 1, each half being independently addressable.

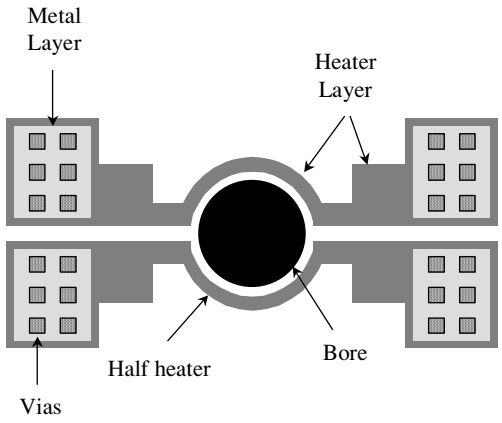

Figure 1. Top view of a nozzle with split heater architecture.

Each nozzle communicates via a fluid channel to a central fluid reservoir. A jet emanates from each nozzle when the fluid reservoir is pressurized. If a small amount of energy (approximately 1 nJ) is applied periodically to the jet by either one or both heater sections, the jet breaks into droplets with uniform volume and velocity and in synchrony with the applied current pulses to the heaters. In addition, if a higher current pulse is applied to one of the semicircular heaters, the droplet formed by that pulse is deflected relative to the unperturbed jet direction by several degrees, depending on the fluid, and geometry of the nozzle. Figure 2 schematically demonstrates the principle of operation of the device.

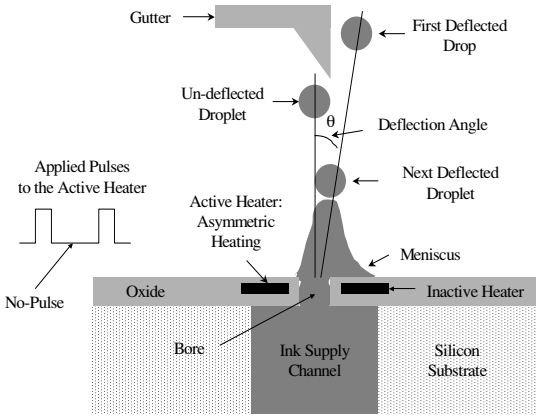

Figure 2. Schematic presentation of the device principle of operation.

To take advantage of low-cost CMOS processing, the nozzle array is fabricated after the completion of the CMOS fabrication steps. Details of two methods are described in [3,4]. A cross-sectional view of the nozzle architecture described in [4] is shown in Fig. 3.

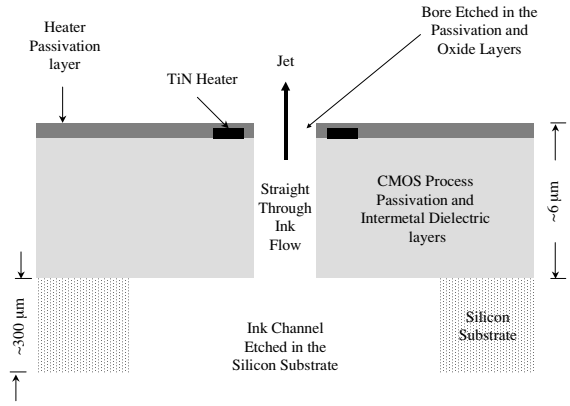

Figure 3. Simplified cross-sectional view of a straight-through fluid flow nozzle architecture.

For this type of nozzle geometry, droplet deflection was small. We show the results for the deflection of 2-propanol in Fig. 4. It is seen that for jet velocities of approximately 8.5 m/s, which is a desired value of operation, the deflection is about 2°. A robust system requires large deflection angles

0-7803-7731-1/03/$17.00 ©2003 IEEE

with minimally applied power and, hence, low temperatures. Furthermore, aqueous-based fluid deflection is typically smaller. Most inks used in consumer applications are aqueous based; therefore, a new nozzle structure was invented that increased deflection substantially, especially for aqueous solutions.

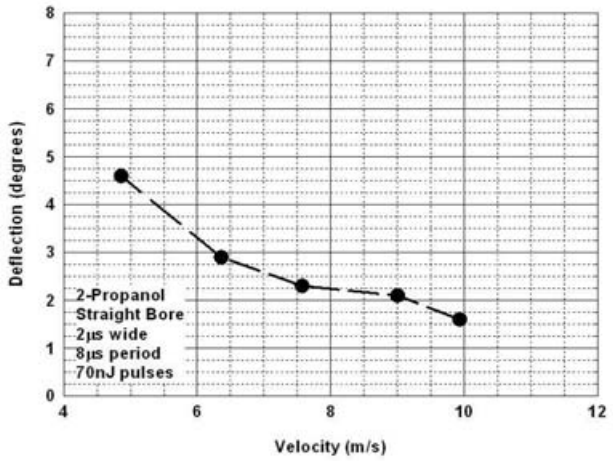

Figure. 4. Jet deflection for 2-Propanol as a function of jet velocity for a nozzle architecture with straight-through fluid flow.

LATERAL FLOW DEVICE

From theoretical analysis, experimental investigation, and finite-difference simulations, we determined that the amount of deflection is controlled by the following three properties of the fluids. First, viscosity variation with temperature causes a momentum imbalance across the exiting jet, resulting in deflection away from the heated side. Second, changes in the surface tension with temperature results in gradients in the local mean curvature and Marangoni stresses (flows tangent to the free surface) that can deflect the jet toward the heated side. And third, the fluid meniscus on the heated side of the orifice pulls in toward the orifice, which results in deflection away from the heated side. From this analysis, we concluded [5] that the nozzle architecture should be altered to maximize one of the above mechanisms. The variation of viscosity with temperature was chosen.

A nozzle architecture that takes advantage of viscosity variation with temperature to cause increased jet deflection is shown in Fig. 5. Its main feature is that the jet exiting the nozzle is formed by the combination of two streams flowing laterally toward the nozzle exit. To accomplish this type of fluid flow, a blockage, marked "Block" in the figure, is constructed so that no direct path exists between the fluid channel and the nozzle exit. The measured jet deflections for 2-propanol and 30% Dowanol DPM in water are shown in Fig. 6 for jet velocities of 8.5 m/s The deflection is increased substantially, compared to the data shown in Fig. 4. The 30% DPM represents a potential aqueous ink solution containing a humectant. The lines through the experimental points are simple polynomial fits. The energy values (abscissa) of Fig. 6 are those applied to the top heater of Fig. 5. The bottom heaters were not activated. The purpose of the bottom heaters is to reduce the energy each heater has to supply so that not one of them is driven to too

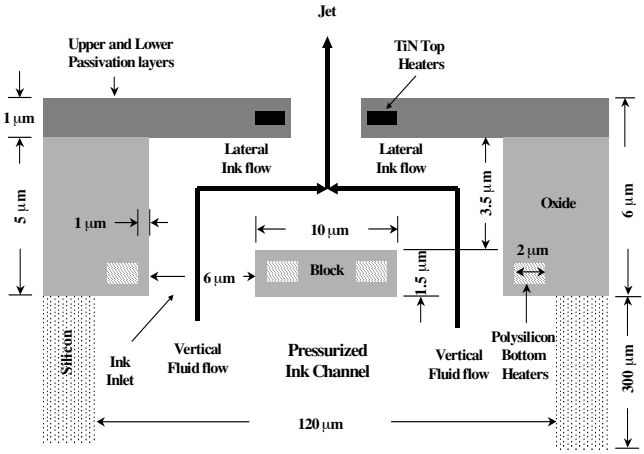

Figure 5. Schematic cross-sectional view of a lateral flow device nozzle with top and bottom heaters. Each one of the heaters may be independently controlled.

high a temperature. One additional observation is that the nozzle architecture in Fig. 3 is much less efficient in transferring heat to the fluid than the nozzle architecture in Fig. 5. The reason for this is that the heater in Fig. 5 rests on a thin oxide membrane while that of Fig. 3 rests on a thick oxide layer that draws heat away from the fluid.

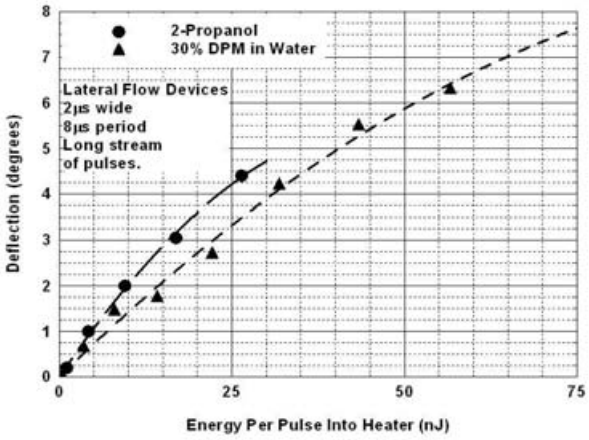

Figure 6. Jet deflection as function of heater energy at a jet velocity of about 8.5 m/s.

We show calculated jet deflections for the same fluids, using a 2-D finite difference simulation (Flow-3D), in Fig. 7. In the simulation, a constant energy (averaged in time) is applied to the heater while pulses were applied in the experiment. The two abscissas can be matched by dividing the experimental energy values given in nanojoules, nJ, by 8 x 10^{-5}, to give milliwatts/μm. For example the 2-propanol experimentally obtained deflection for 30 nJ is about 4.6 degrees while the simulation result for 3.75 milliwatts/μm is approximately 6.5 degrees.

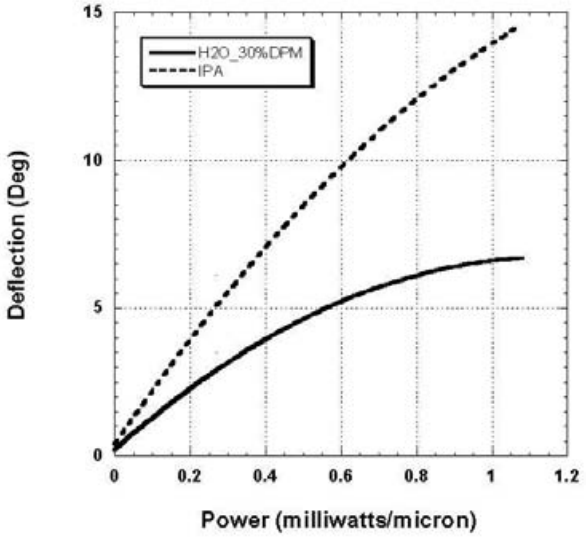

Figure. 7. 2-D simulation results of jet deflection as a function of heater energy at a jet velocity of 8.5 m/s.

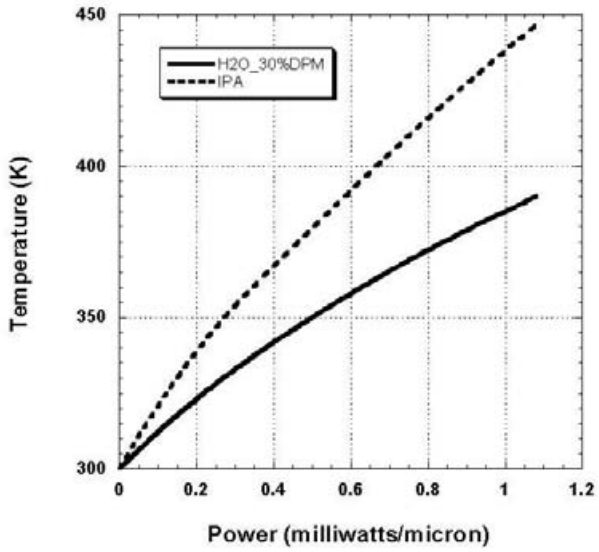

Figure 8. Calculated fluid temperature just below the heater as a function of heater energy.

The theoretical analysis also helps explain the higher deflection for 2-propanol compared to 30% DPM in water. Recall that the major factor causing the deflection is the change in viscosity as a function of temperature, which, in turn, increases the momentum of the fluid under the nozzle plate on the heated side. However, the change in viscosity with temperature is about equal for the two fluids. Of the two fluids, 2-propanol has lower thermal conductivity and heat capacity. Thus, its temperature change, as shown in Fig. 8, is higher for the same heater energy. The higher temperature change results in a larger change in viscosity, thus a higher momentum difference between the two converging lateral streams, yielding more deflection.

We also fabricated nozzles identical to those in Fig. 5 but without the "Block." Jet deflection as a function of heater energy for these devices is shown in Fig. 9. The deflection is much larger compared to nozzles of the type shown in Fig. 3. The improvement is attributable to substantial lateral fluid flow, even with the blocking structure absent. This is confirmed by modelling results.

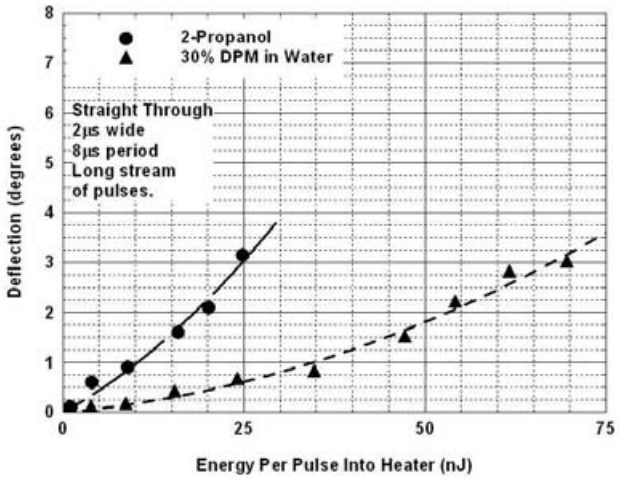

Figure 9. Jet deflection for a nozzle identical to that shown in Fig. 5 except without the "Block."

FABRICATION

Single lateral flow nozzles were fabricated using silicon VLSI technology and MEMS fabrication techniques. Fabrication of arrays of such nozzles on standard CMOS wafers containing the logic and drive circuits [6] are in process. Following is the fabrication sequence for lateral flow nozzles on wafers that have not gone through a CMOS process.

(Steps 1-12 would normally be part of the CMOS process)

1) Grow thermal oxide 4000 A.
2) Low-pressure chemical vapor deposition (LPVCD) doped polysilicon 4000A.
3) Define bottom heaters. Dry etch 4000A Poly using chlorine chemistry.
4) Thermal oxidation of polysilicon heater (500 A oxide).
5) Deposit LPCVD TEOS ($Si(OC_2H_5)_4$) 2000A.
6) Deposit LPCVD borophosphosilicate glass (BPSG) 5000A.
7) Define and open contacts to Poly heaters.
8) Sputter TiW/Al (2000A/6000A) for electrical interconnect.
9) Define and dry etch TiW/Al using chlorine chemistry.
10) Deposit 5 µm PECVD oxide.
11) Chemical mechanical polishing (CMP) of oxide (remove approximately 1 µm).

12) Define fluid inlets and partially dry etch oxide, 1.5 µm.

(Steps 13-30 MEMS portion of the process)

13) Define blocks and dry etch remaining oxide, 3.5 µm, to reach the Silicon surface at the inlets.
14) Coat, expose, develop, and bake 10 µm polyimide.
    - Polyimide HD8000 by HD Microsystems
15) CMP polyimide using Cabot W-A400 slurry (Al_2O_3).
    - Tool by Strausbaugh model 6EC Planarizer.
    - Two steps: Removal rate: 5.5 µm/minute and 0.5 µm/minute.
16) Megasonic bath clean to remove CMP slurry. H_2O: H_2O_2: NH_4OH 40:2:1
17) Deposit bottom passivation layers PECVD TEOS/ Nitride/ TEOS (2500A/ 2000A/ 2500A).
18) Sputter Ti/TiN (50A/600A) as top heater material.
19) Define and dry etch Ti/TiN top heaters using fluorine chemistry.
20) Deposit PECVD TEOS/Nitride (1500A/1500A).
21) Define and open contacts to TiN heaters.
22) Sputter Al (6000A) for electrical interconnect.
23) Define and dry etch Al using chlorine chemistry.
24) Deposit 3000A PECVD Nitride top passivation layer.
25) Define and etch nozzle bore by dry etching Nitride/ Oxide/ Oxide/ Nitride/ Oxide stack (4500A/ 1500A/ 2500A/ 2000A/ 2500A).
26) Define and open contact to bond pads by dry etching dielectric stack.
27) Thin wafer down to 300 µm.
    - Tool by Strausbaugh model 7AA-II
    - Removal rate: 150 µm/minute.
28) Define fluid channels in the backsides of wafers.
29) Etch through wafer with STS tool using Bosch process.
30) Remove sacrificial polyimide using oxygen chemistry.

An SEM of a finished device is shown in Fig. 10.

CONCLUSIONS

We described the architecture and fabrication of a fluidic device with increased droplet deflection. Using a flow-directing block in the fluid chamber results in more control of the lateral momentum of the converging streams. The device is capable of producing precise picoliter size droplets and steering them. The precision is a consequence of the reproducibility of the nozzles, which are made using VLSI technology and tools. In addition, the droplet size is determined by the precise timing of applied heat pulses.

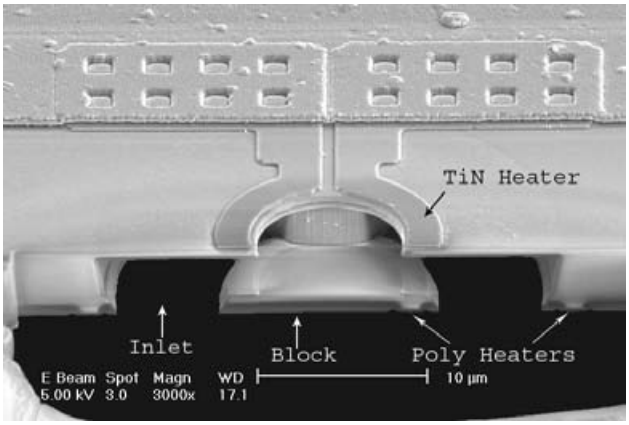

Figure 10. SEM image of a finished device that has been cut by a focused ion beam.

ACKNOWLEDGEMENTS

We would like to thank the Eastman Kodak Company R&D MEMS fabrication facility for making these devices.

References

[1] J.M. Chwalek, D.P. Trauernicht, C.N. Delametter, D.L. Jeanmaire, and C.N. Anagnostopoulos, "Novel Silicon-Based Continuous Inkjet Printhead Employing Asymmetric Deflection Means," Proc. IS&T NIP17: Int. Conf. on Digital Printing Technologies, Sept. 30–Oct. 5, 2001, Fort Lauderdale FL, pp. 291-294.

[2] D.P. Trauernicht, C.N. Delametter, J.M. Chwalek, D.L. Jeanmaire, and C.N. Anagnostopoulos, "Performance of Fluids in Silicon-Based Continuous Inkjet Printhead Using Asymmetric Heating," Proc. IS&T NIP17: Int. Conf. on Digital Printing Technologies, Sept. 30–Oct. 5, 2001, Fort Lauderdale FL, pp. 295-298.

[3] 3. C.N. Anagnostopoulos, J.A. Lebens, G.A. Hawkins, D.P. Trauernicht, J.M. Chwalek, and C.N. Delametter, "CMOS/MEMS Integrated Ink Jet Print Head with Heater Elements Formed During CMOS Processing and Method of Forming Same," U.S. Patent 6,450,619, Issued Sept. 17, 2002

[4] A. Witvrouw, B. Parmentier, K. Baert, L. Haspeslagh, P. De Moor, A. Verbist, E. Rosseel, C. Anagnostopoulos, G. Hawkins, J. Chwalek, D. Trauernicht, and J. Lebens, "High Resolution, Large Width Ink Jet Print Head made by CMOS Post-Processing," Submitted for publication to IEEE J. MicroElectroMechanical Systems.

[5] C.N. Delametter, J.M. Chwalek, and D.P. Trauernicht, "Deflection Enhancement for Continuous Ink Jet printers," U.S. Patent 6,497,510, Issued Dec. 24, 2002

[6] C.N. Anagnostopoulos, J.A. Lebens, and C.N. Delametter, "CMOS/MEMS Integrated Ink Jet Print Head with Oxide Based Lateral Flow Nozzle Architecture and Method of Forming Same," US Patent 6,382,782, Issued May 7, 2002.